

# Targeted free energy perturbation revisited: Accurate free energies from mapped reference potentials

Andrea Rizzi,<sup>1, 2</sup> Paolo Carloni,<sup>1, 3, 4, \*</sup> and Michele Parrinello<sup>2, †</sup>

<sup>1</sup>*Computational Biomedicine, Institute of Advanced Simulations IAS-5/Institute for Neuroscience and Medicine INM-9, Forschungszentrum Jülich GmbH, Jülich 52428, Germany*

<sup>2</sup>*Atomistic Simulations, Italian Institute of Technology, Via Morego 30, Genova 16163, Italy*

<sup>3</sup>*Molecular Neuroscience and Neuroimaging (INM-11),*

*Forschungszentrum Jülich GmbH, Jülich 52428, Germany*

<sup>4</sup>*Department of Physics, RWTH Aachen University, Aachen 52074, Germany*

(Dated: October 7, 2021)

We present an approach that extends the theory of targeted free energy perturbation (TFEP) to calculate free energy differences and free energy surfaces at an accurate quantum mechanical level of theory from a cheaper reference potential. The convergence is accelerated by a mapping function that increases the overlap between the target and the reference distributions. Building on recent work, we show that this map can be learned with a normalizing flow neural network, without requiring simulations with the expensive target potential but only a small number of single-point calculations, and, crucially, avoiding the systematic error that was found previously. We validate the method by numerically evaluating the free energy difference in a system with a double-well potential and by describing the free energy landscape of a simple chemical reaction in the gas phase.

*Introduction.*—Predicting free energy changes is one of the fundamental problems in physics and chemistry with countless applications to drug development, biology, and materials science [1]. Molecular simulations provide a rigorous means of determining this property. On one hand, endpoint and alchemical approaches [2, 3] calculate free energy differences  $\Delta f$  between two states (e.g., binding and solvation free energies) or two different molecules (e.g., the change in affinity between two drugs towards their target receptor). On the other, methods such as umbrella sampling [4, 5] (US), metadynamics [6–8] (MetaD), and adaptive biasing force [9, 10] allow reconstructing the free energy surface (FES) of a system as a function of one or more physical collective variables (CVs), also known as potential of mean force.

In both classes of methods, a full or partial quantum mechanical (QM) representation of the system is often desirable. For instance, hybrid molecular mechanics/quantum mechanics potential energy surfaces based on post-Hartree-Fock, density functional theory (DFT), or quantum machine learning potentials [11–13] have been used to overcome some of the shortcomings of empirical and semi-empirical calculations to study ligand binding [14–18] and chemical reactions [19–22]. However, the use of accurate quantum chemical methods severely limits the size of the system that can be studied.

In this respect, using a cheaper potential as a reference and recovering the accuracy of a more expensive Hamiltonian with free energy perturbation (FEP) [23] may achieve significant computational savings. Indeed, only a relatively small number of expensive energy calculations are required to achieve the accuracy of the target level of theory. This approach was pioneered by Gao [24] and by Muller and Warshel [25] for the calculations of  $\Delta f$  and FES, respectively. However, the speed of con-

vergence of FEP degrades rapidly as the overlap between the reference and target distributions decreases, restricting its applicability [21, 26].

To overcome this problem, several  $\Delta f$  and FES methods have been successfully developed so as to avoid extensive simulations of the full system with the target Hamiltonian. These either use a sequence of intermediate Hamiltonians [14, 27], or employ highly efficient estimators [15, 28], or train cheaper and *ad-hoc* parametrized models for either the reference [16, 21, 22] or the target potential [29–31]. An elegant approach to the calculation of  $\Delta f$  was introduced by Jarzynski in 2002 under the name of targeted free energy perturbation (TFEP) [32, 33]. The method performs a mapping of the atomic coordinates such that the overlap between reference and target distributions is increased. An advantage of TFEP over existing methods is that, in principle, it enables instantaneous convergence of the free energy difference. Moreover, the mapped configurations can also be used to study the molecular geometries at the target level of theory. Because this mapping is generally very complex, it has been suggested to represent it with a neural network (NN) [34]. Unfortunately, such NN was found to introduce a systematic error in the  $\Delta f$  unless it was also trained with samples obtained from extensive simulations using the target Hamiltonian. In the context of reference potential methods, however, this defeats the purpose of employing a cheaper Hamiltonian.

In this Letter, we revisit TFEP and the formulation of the learning problem proposed in Ref. [34], we find the origin of the difficulty, derive a rigorous bound that explains the systematic error reported and, above all, offer a solution. As a result, we are able to learn an efficient Jarzynski mapping with a small set of expensive calculations. Next, we validate the methodology numerically on

a simple, double-well potential system. Finally, we extend the method to the calculation of the FES and test it by simulating a simple chemical reaction in the gas phase.

*Computing free energy differences.*—Consider the problem of determining the free energy difference between a reference (or sampled) distribution  $A$  and a target distribution  $B$ , which is given by

$$\Delta f_{AB} = -\log \frac{Z_B}{Z_A} = -\log \frac{\int_{\Gamma_B} e^{-u_B(\mathbf{y})} d\mathbf{y}}{\int_{\Gamma_A} e^{-u_A(\mathbf{x})} d\mathbf{x}}, \quad (1)$$

where for convenience we have expressed all energies in units of  $k_B T$ , and  $Z_A$ ,  $\Gamma_A$ , and  $u_A(\mathbf{x})$  are the configurational partition function, the domain of integration, and the reduced potential energy, respectively, of configuration  $\mathbf{x}$  associated with the Boltzmann distribution  $A$

$$p_A(\mathbf{x}) = \frac{e^{-u_A(\mathbf{x})}}{Z_A}. \quad (2)$$

When  $\Gamma_A = \Gamma_B$ , Eq. (1) can be computed using only samples from  $A$  through the Zwanzig identity [23]

$$\Delta f_{AB} = -\log \langle e^{-w_{AB}(\mathbf{x})} \rangle_A, \quad (3)$$

where  $\langle g(\mathbf{x}) \rangle_A = \int_{\Gamma_A} p_A(\mathbf{x}) f(\mathbf{x}) d\mathbf{x}$  and  $w_{AB}(\mathbf{x}) = u_B(\mathbf{x}) - u_A(\mathbf{x})$ .

Jarzynski's TFEP derivation [32] is based on an invertible transformation  $\mathcal{M} : \Gamma_A \rightarrow \Gamma_B$  that maps samples from  $A$  to a different ensemble  $A'$  that shares a larger overlap with  $B$ . We provide here an alternative derivation and interpretation of TFEP that considers the map  $\mathcal{M}$  as transforming the target distribution  $B$  rather than  $A$ . Specifically, we exploit the observation of Zhu *et al.* [35], who noticed that performing a change of variable through  $\mathbf{y} = \mathcal{M}(\mathbf{x})$  leads to a new Boltzmann distribution  $B'$  defined on  $\Gamma_A$  with an effective potential

$$u_{B'}(\mathbf{x}) = u_B(\mathcal{M}(\mathbf{x})) - \log |J_{\mathcal{M}}(\mathbf{x})|, \quad (4)$$

where  $|J_{\mathcal{M}}|$  is the absolute value of the Jacobian determinant of  $\mathcal{M}$ . Moreover, being a change of variable, the transformation preserves the partition function (i.e.,  $Z_{B'} = Z_B$ ). The problem in Eq. (1) is thus equivalent to computing  $\Delta f_{AB'} = -\log Z_{B'}/Z_A$  for a convenient choice of  $B'$ . We can then recover the TFEP estimator [32] by simply using FEP on  $A$  and  $B'$

$$\Delta \hat{f}_{AB}(D) = -\log \frac{1}{N} \sum_i^N e^{-w_{AB'}(\mathbf{x}_i)}, \quad (5)$$

where  $D = \{\mathbf{x}_i\}$  is a dataset of  $N$  samples from  $p_A(\mathbf{x})$ . Eq. (5) is valid for any invertible  $\mathcal{M}$ , but an optimal choice is the one  $\mathcal{M}^*$  that maps  $B$  into a distribution  $B^*$  that overlaps perfectly with  $A$ , i.e.,

$$p_{B^*}(\mathbf{x}) = p_A(\mathbf{x}). \quad (6)$$

With  $\mathcal{M}^*$  at hand, one can calculate from Eq. (2) and (6) the free energy difference  $\Delta f_{AB}$  as

$$\Delta f_{AB} = w_{AB^*}(\mathbf{x}). \quad (7)$$

A remarkable feature of this relation is that, at least in principle, a single sample is sufficient to obtain a converged estimate of  $\Delta f_{AB}$ .

Following Ref. [34], we implement the map with a suitably trained normalizing flow neural network [36]. Normalizing flows are particularly suited for this problem since they lead by construction to maps that are invertible and whose Jacobian (see Eq. (4)) can be computed cheaply. The parameters  $\boldsymbol{\theta}^*$  of the NN representing the optimal map  $\mathcal{M}^*$  are obtained by minimizing the Kullback-Leibler (KL) divergence  $D_{\text{KL}}[p_A || p_{B^*}]$ , which, using Eq. (2), can be written as

$$D_{\text{KL}}[p_A || p_{B^*}] = \langle w_{AB^*}(\mathbf{x}; \boldsymbol{\theta}) \rangle_A - \Delta f_{AB}. \quad (8)$$

In Ref. [34],  $\Delta \hat{f}_{AB}$  is then computed with the optimized map on the same dataset used to train the NN. This choice was motivated by the goal of reducing the amount of data needed.

Here, we show that such a procedure leads to a systematic error. To this end, let us first recast the learning problem as a maximum likelihood (ML) estimation. Given a set  $D_{\text{tr}}$  of  $N_{\text{tr}}$  independent samples from  $p_A$ , we use Eq. (6) and (4) to write the probability of observing the data as

$$p_A(D_{\text{tr}}) = \prod_i^{N_{\text{tr}}} p_{B^*}(\mathbf{x}_i) \propto \prod_i^{N_{\text{tr}}} e^{-u_B(\mathcal{M}^*(\mathbf{x}_i)) + \log |J_{\mathcal{M}}(\mathbf{x}_i)|}. \quad (9)$$

After simple manipulations, the negative log-likelihood reads:

$$\mathcal{L}(\boldsymbol{\theta}) = \frac{1}{N_{\text{tr}}} \sum_i^{N_{\text{tr}}} w_{AB^*}(\mathbf{x}_i; \boldsymbol{\theta}). \quad (10)$$

The expression in Eq. (10) is, within an immaterial constant, how the KL divergence in Eq. (8) is estimated using a finite sample. In the limit of  $N_{\text{tr}} \rightarrow \infty$ ,  $\mathcal{L}(\boldsymbol{\theta})$  approaches the true value of the KL divergence, and the ML solution  $\boldsymbol{\theta}^{\text{ML}}$  is identical to the perfect map  $\boldsymbol{\theta}^*$ . In general, however, with a finite sample we have by definition  $\mathcal{L}(\boldsymbol{\theta}^*) \geq \mathcal{L}(\boldsymbol{\theta}^{\text{ML}})$ . Thus, using Eq. (7) and Jensen's inequality we finally obtain the inequality

$$\Delta f_{AB} \geq \Delta \hat{f}_{AB}(D_{\text{tr}}; \boldsymbol{\theta}^{\text{ML}}). \quad (11)$$

This is the cause for the systematic error observed in Ref. [34]. Eq. (11) predicts that if the free energy estimate is computed on the training dataset, it converges systematically to an incorrect value as the training increases. Such error can thus be interpreted as a peculiar case of overfitting that results in performance degradation on the training set.

To solve this problem, instead of using samples from the target distribution as in Ref. [34], we note that Eq. (11) is a consequence of the dependence of  $\theta^{\text{ML}}$  on  $D_{\text{tr}}$ . Thus, the issue vanishes if  $\Delta\hat{f}_{AB}$  is computed using an *independent* set of configurations. Indeed, given such an evaluation dataset  $D_{\text{ev}}$  of  $N_{\text{ev}}$  samples, by applying Jensen's inequality to Eq. (5) we recover the bound [33]

$$\langle \Delta\hat{f}_{AB}(D_{\text{ev}}; \theta) \rangle \geq \Delta f_{AB}, \quad (12)$$

where the mean is intended over all possible instances of  $D_{\text{ev}}$ . Eq. (12) is valid for any map  $\theta$ , including  $\theta^{\text{ML}}$ , and the equality is approached for  $N_{\text{ev}} \rightarrow \infty$ .

Note that a systematic error is present also when using the evaluation set but only on average rather than on *all* training datasets as in Eq. (11). Moreover, we expect the error on  $D_{\text{tr}}$  to increase in the low-data regimes typical of molecular simulations, where only a few thousand independent data points can be used for training, and the effects of overfitting are more pronounced. Thus, in practice, we expect to obtain smaller errors and more robust estimates of the uncertainty of  $\Delta\hat{f}_{AB}$  on an independent set than on  $D_{\text{tr}}$ .

We check the validity of our method by computing the  $\Delta f_{AB}$  between the two double-well potential distributions in Fig. 1. We implemented the parametric map with an inverse autoregressive flow (IAF) [37, 38]. For each tested training dataset size  $N_{\text{tr}}$ , we trained 40 NNs on randomly-generated datasets and evaluated each net-

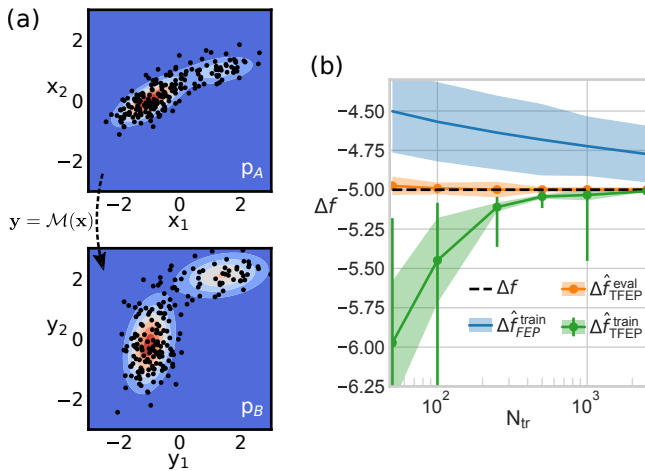


FIG. 1. Calculation of  $\Delta f_{AB}$  on a 2D free energy landscape. (a) Contour plots of the sampled (A, top) and target (B, bottom) distributions. The overlaid black dots were sampled from  $p_A$  (top) and mapped through the trained  $M$  (bottom). (b) Theoretical free energy difference (dashed, black) or computed on the evaluation dataset ( $N_{\text{ev}} = 100$ ) with TFEP (orange) and on the training set with TFEP (green) or FEP (blue). Lines, shaded areas, and (for  $\Delta f_{\text{TFEP}}^{\text{train}}$ ) error bars represent the average, standard deviation, and the full range of the predictions across repeats, respectively. The energy values are in units of  $k_B T$ .

work on independent datasets of constant size  $N_{\text{ev}} = 100$ . We refer the reader to the Supplemental Material [39] for the technical details of all the numerical experiments in this work.

As predicted by Eq. (11), every single NN underestimated  $\Delta f_{AB}$  on  $D_{\text{tr}}$ , and, counterintuitively, overfitting resulted in significantly worse performance on the training rather than the independent set, especially when  $D_{\text{tr}}$  was small. In contrast, in spite of its small size ( $N_{\text{ev}} = 100$ ), evaluating  $\Delta\hat{f}_{AB}$  on the evaluation sets consistently outperformed both standard FEP and TFEP on  $D_{\text{tr}}$ . The data in Fig. 1 support the conclusion that it is beneficial to reduce the amount of data available for training to allow the calculation of  $\Delta\hat{f}_{AB}$  on a set of independent configurations.

*Computing free energy surfaces.*—Here, we show how TFEP theory can be extended to determine the free energy surface  $f_B(\mathbf{s})$  as a function of a generally multidimensional CV  $\mathbf{s}$ . We do so by adding to  $f_A(\mathbf{s})$ , which is estimated using a cheap reference potential, the perturbation term

$$\Delta f_{AB}(\mathbf{s}) = -\log \frac{Z_B(\mathbf{s})}{Z_A(\mathbf{s})} = -\log \langle e^{-w_{AB}(\mathbf{x})} \rangle_{A|\mathbf{s}}, \quad (13)$$

where  $Z_B(\mathbf{s}) = \int_{\Gamma_B} e^{-u_B(\mathbf{y})} \delta[\mathbf{s}(\mathbf{y}) - \mathbf{s}] d\mathbf{y}$  is the partition function restricted to  $\mathbf{s}$ , and the average is taken over the distribution

$$p_A(\mathbf{x}|\mathbf{s}) = \frac{e^{-u_A(\mathbf{x})}}{Z_A(\mathbf{s})} \delta[\mathbf{s}(\mathbf{x}) - \mathbf{s}]. \quad (14)$$

First, note that simply plugging in Eq. (13) the optimal TFEP map  $M^*$ , using Eq. (7), results in the incorrect expression  $\Delta f_{AB}(\mathbf{s}) = \Delta f_{AB}$ . Indeed, to formulate an equivalent problem in terms of the transformed distribution  $B'$ , the change of variable must now preserve the value of  $Z_B(\mathbf{s})$ . To achieve this, a sufficient condition is that the transformation  $M_s : \Gamma_A \rightarrow \Gamma_B$  satisfies

$$s(M_s(\mathbf{x})) = s(\mathbf{x}). \quad (15)$$

The relation in Eq. (15) prevents  $M_s$  from moving probability density along  $\mathbf{s}$  so that  $p_B(\mathbf{s}) = Z_B(\mathbf{s})/Z_B$  (i.e., the equilibrium distribution of the CV) is maintained, and  $M_s$  transforms only the degrees of freedom orthogonal to  $\mathbf{s}$ , which are distributed according to  $p_B(\mathbf{x}|\mathbf{s})$ . Similarly to TFEP, to maximize the overlap and achieve instantaneous convergence, the optimal map  $M_s^*$  transforms  $p_B(\mathbf{x}|\mathbf{s}) \rightarrow p_A(\mathbf{x}|\mathbf{s})$  for all values of  $\mathbf{s}$ , which implies  $w_{AB^*}(\mathbf{x}) = \Delta f_{AB}(\mathbf{s})$ .

The derivation and characterization of the learning problem for  $M_s^*$  follow arguments similar to those used above for TFEP and it is detailed in the Supplemental Material [39]. We discuss here the main results. The first is that  $M_s^*$  can be learned by minimizing the same log-likelihood in Eq. (10) with the key difference that the samples in the training dataset can be obtained from

simulations employing an arbitrary biasing potential of the form  $V(\mathbf{s})$ . This has two crucial consequences: (i) it enables the use of CV-based enhanced sampling techniques in the reference simulation; (ii) it allows allocating more data points in the training dataset to areas of the CV that would be otherwise poorly represented like, for instance, transition states. In our experience, both are critical to obtain an improved free energy surface across the whole range of  $\mathbf{s}$ .

The second is that the following estimator for  $\Delta f_{AB}(\mathbf{s})$  can be derived for reference simulations performed with umbrella sampling and metadynamics

$$\Delta \hat{f}_{AB}(\mathbf{s}, D) = -\log \frac{\sum_i \alpha_i e^{-w_{AB'}(\mathbf{x}_i)} \delta[\mathbf{s}(\mathbf{x}_i) - \mathbf{s}]}{\sum_i \alpha_i \delta[\mathbf{s}(\mathbf{x}_i) - \mathbf{s}]}, \quad (16)$$

where the weights  $\alpha_i$  take different values depending on whether US, MetaD, or no biasing potential was used. The third and final result is that the maximum-likelihood map is subject to systematic error when  $\Delta \hat{f}_{AB}(\mathbf{s}, D)$  is evaluated on the training dataset according to

$$\sum_s \frac{N_s}{N_{\text{tr}}} \Delta f_{AB}(\mathbf{s}) \geq \sum_s \frac{N_s}{N_{\text{tr}}} \Delta \hat{f}_{AB}(\mathbf{s}, D_{\text{tr}}; \theta^{\text{ML}}), \quad (17)$$

where  $N_s = \sum_i^{N_{\text{tr}}} \delta[\mathbf{s}(\mathbf{x}_i) - \mathbf{s}]$  is the number of samples in bin  $\mathbf{s}$ , and the summation goes over all bins. Note that the implications of Eq. (17) are slightly different from TFEP (see Eq. (11)). In particular, Eq. (17) states that overfitting causes the free energy surface to be underestimated on  $D_{\text{tr}}$  in an average sense. As a result, fortuitous cancellation/amplification of error may arise when the FES thus obtained is used to compute free energy differences along  $\mathbf{s}$ .

We now test the methodology by investigating a simple reaction, the S<sub>N</sub>2 reaction  $\text{CH}_3\text{F} + \text{Cl}^- \rightarrow \text{CH}_3\text{Cl} + \text{F}^-$  in vacuo. We evaluated the FES of the reaction at a relatively high level of theory (MP2) from reference data based on semi-empirical PM6 calculations [40]. Four independent 100 ns simulations were performed with well-tempered MetaD [6, 7]. As with any CV-based methodology, the choice of the collective variable is critical. Here, we use a linear combination of the C-F and C-Cl distances, which was shown to describe well this reaction [19].

Fig. 2(a) shows the convergence speed of standard and targeted FEP in computing the free energy barrier  $\Delta f^{(\text{F} \rightarrow \text{Cl})}$  [41, 42] and the free energy difference between products and reactants  $\Delta f_{\text{ClF}}$ . Thus, the precision of the estimates can visibly improve on the evaluation dataset even after a single epoch of training in low-data regimes ( $N_{\text{tr}} = 1428$ ). The learning efficiency is largely a consequence of the reference potential already providing a very good approximation to the target. Therefore, if the parameters of the NN are initialized so that the map equals the identity function, the training starts already close to

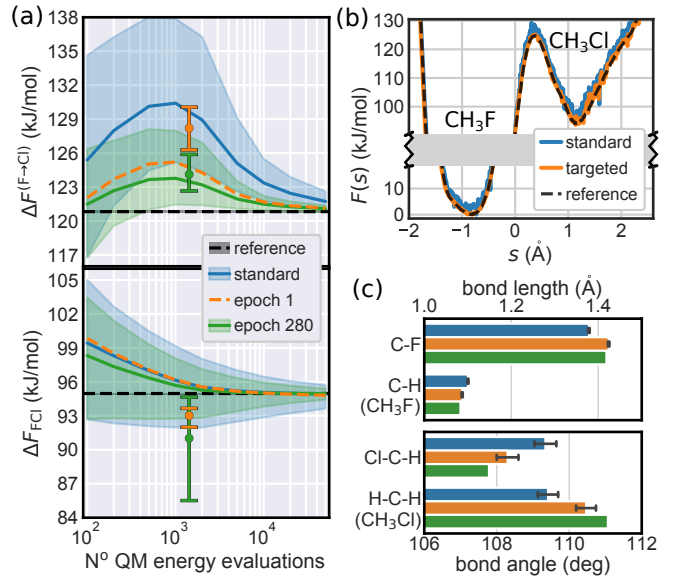


FIG. 2. (a) Free energy barrier (top) and free energy difference (bottom) for the S<sub>N</sub>2 reaction as a function of the number of MP2 energy evaluations computed with standard (blue) and targeted reweighting after 1 (orange) and 280 (green) epochs of training. Lines and shaded areas represent means and 95% confidence intervals obtained by bootstrapping over the evaluation set. Dots and error bars were instead computed on 50 different training sets. (b) Free energy profile along  $s$ . (c) Comparison of the average bond lengths (top) and angles (bottom) between the simulated (blue), mapped (orange), and MP2-optimized geometries (green).

a good solution. On the other hand, rapidly approaching the maximum-likelihood map also means that the effect of overfitting is apparent very soon, and indeed the systematic error on the training set visibly exceeded that on  $D_{\text{ev}}$  after only a single epoch of training.

Due to the asymmetric free energy profile, only approximately 1/5 of the configurations represented the CH<sub>3</sub>Cl state in the training and evaluation datasets (see Fig. 2(b)). In addition, we observed that the fluoride ion energetic interactions with the CH<sub>3</sub>Cl hydrogens were much stronger when using PM6 than with MP2, which decreased the overlap between the two Hamiltonians. As a result, the FES converged more rapidly for the CH<sub>3</sub>F state than for CH<sub>3</sub>Cl. To prioritize instead the analysis of high free energy states, one can change the biasing potential employed in the simulation or subsample the trajectory to allocate more data points to the desired areas of the FES.

To verify that the learned map did capture the physics of the target Hamiltonian, we compared the mapped configurations to those obtained by performing geometry optimization at the MP2 level of theory. We found that only a few average bond lengths and angles (shown in Fig. 2(c)) were changed by the mapping with any statistical significance, and in all cases, the NN pushed the av-

erage structures closer to the MP2-optimized ones. While we are aware that the anharmonic thermal fluctuations of bond lengths and angles sampled during the simulation prevent an exact comparison to the MP2-optimized structures, the trend is quite apparent.

*Outlook.*—In this Letter, we showed how NN-based mapping functions can be used to improve the accuracy and convergence of free energy differences and FES estimates starting from a (possibly biased) reference potential. A key contribution is the characterization of the systematic error caused by overfitting, which effectively enables the application of TFEF theory with maps trained solely from the reference distribution. The work paves the way for further applications of this methodology to different problems (e.g., binding, enzymatic reactions) with any pair of Hamiltonians (e.g., force fields and NN-based potentials). Moreover, the method could in principle be exploited to study transition state geometries at higher levels of theory.

A challenge in computing the FES with this methodology is the implementation of the CV-preserving condition in Eq. (15). While this is relatively easy to enforce in the NN architecture for simple geometric CVs commonly used, for example, in (bio)chemical reactions [21, 43, 44], it is not obvious how to realize it efficiently with highly nonlinear variables such as those based on neural networks [45–48]. Further work will be needed to investigate how this condition can be relaxed or approximated to extend the applicability of the method to such cases.

AR would like to thank GiovanniMaria Piccini and Emiliano Ippoliti for valuable advice concerning the setup of the semi-empirical and QM calculations. The authors gratefully acknowledge the computing time granted through JARA on the supercomputer JURECA-DC [49] at Forschungszentrum Jülich (Project ID: trp2020) and the computational resources provided by RWTH Aachen University. The project received funding from the Helmholtz European Partnering program ("Innovative high-performance computing approaches for molecular neuromedicine"). PC acknowledges financial support from Deutsche Forschungsgemeinschaft via the Research Unit FOR2518 "Functional Dynamics of Ion Channels and Transporters – DynIon", project P6. PC also acknowledges the Human Brain Project funded by the European Union's Horizon 2020 Framework Programme for Research and Innovation under the Specific Grant Agreement No. 945539 (Human Brain Project SGA3).

(Springer, Berlin, Heidelberg, 2007).

- [2] E. Wang, H. Sun, J. Wang, Z. Wang, H. Liu, J. Z. Zhang, and T. Hou, End-point binding free energy calculation with mm/pbsa and mm/gbsa: strategies and applications in drug design, *Chem. Rev.* **119**, 9478 (2019).
- [3] A. S. Mey, B. K. Allen, H. E. B. Macdonald, J. D. Chodera, D. F. Hahn, M. Kuhn, J. Michel, D. L. Mobley, L. N. Naden, S. Prasad, *et al.*, Best practices for alchemical free energy calculations [article v1. 0], *Living J. Comp. Mol. Sci.* **2**, 18378 (2020).
- [4] G. M. Torrie and J. P. Valleau, Nonphysical sampling distributions in monte carlo free-energy estimation: Umbrella sampling, *J. Comput. Phys.* **23**, 187 (1977).
- [5] M. Souaille and B. Roux, Extension to the weighted histogram analysis method: combining umbrella sampling with free energy calculations, *Comput. Phys. Commun.* **135**, 40 (2001).
- [6] A. Laio and M. Parrinello, Escaping free-energy minima, *Proc. Natl. Acad. Sci. U.S.A.* **99**, 12562 (2002).
- [7] A. Barducci, G. Bussi, and M. Parrinello, Well-tempered metadynamics: a smoothly converging and tunable free-energy method, *Phys. Rev. Lett.* **100**, 020603 (2008).
- [8] M. Invernizzi and M. Parrinello, Rethinking metadynamics: from bias potentials to probability distributions, *J. Phys. Chem. Lett.* **11**, 2731 (2020).
- [9] E. Darve and A. Pohorille, Calculating free energies using average force, *J. Chem. Phys.* **115**, 9169 (2001).
- [10] J. Hénin and C. Chipot, Overcoming free energy barriers using unconstrained molecular dynamics simulations, *J. Chem. Phys.* **121**, 2904 (2004).
- [11] J. Behler and M. Parrinello, Generalized neural-network representation of high-dimensional potential-energy surfaces, *Phys. Rev. Lett.* **98**, 146401 (2007).
- [12] K. T. Schütt, H. E. Sauceda, P.-J. Kindermans, A. Tkatchenko, and K.-R. Müller, Schnet—a deep learning architecture for molecules and materials, *J. Chem. Phys.* **148**, 241722 (2018).
- [13] J. S. Smith, B. T. Nebgen, R. Zubatyuk, N. Lubbers, C. Devereux, K. Barros, S. Tretiak, O. Isayev, and A. E. Roitberg, Approaching coupled cluster accuracy with a general-purpose neural network potential through transfer learning, *Nat. Commun.* **10**, 1 (2019).
- [14] M. Wang, Y. Mei, and U. Ryde, Host–guest relative binding affinities at density-functional theory level from semiempirical molecular dynamics simulations, *J. Chem. Theory Comput.* **15**, 2659 (2019).
- [15] E. C. Dybeck, G. Konig, B. R. Brooks, and M. R. Shirts, Comparison of methods to reweight from classical molecular simulations to qm/mm potentials, *J. Chem. Theory Comput.* **12**, 1466 (2016).
- [16] P. S. Hudson, K. Han, H. L. Woodcock, and B. R. Brooks, Force matching as a stepping stone to qm/mm cb [8] host/guest binding free energies: a sampl6 cautionary tale, *J. Comput. Aided Mol. Des.* **32**, 983 (2018).
- [17] R. Capelli, W. Lyu, V. Bolnykh, S. Meloni, J. M. H. Olsen, U. Rothlisberger, M. Parrinello, and P. Carloni, Accuracy of molecular simulation-based predictions of  $k_{\text{off}}$  values: A metadynamics study, *J. Phys. Chem. Lett.* **11**, 6373 (2020).
- [18] D. A. Rufa, H. E. B. Macdonald, J. Fass, M. Wieder, P. B. Grinaway, A. E. Roitberg, O. Isayev, and J. D. Chodera, Towards chemical accuracy for alchemical free energy calculations with hybrid physics-based machine learning/molecular mechanics potentials (2020), bioRxiv

\* p.carloni@fz-juelich.de

† michele.parrinello@iit.it

[1] C. Chipot and A. Pohorille, *Free energy calculations*

(unpublished).

[19] G. Piccini and M. Parrinello, Accurate quantum chemical free energies at affordable cost, *J. Phys. Chem. Lett.* **10**, 3727 (2019).

[20] J. Sirirak, N. Lawan, M. W. Van der Kamp, J. N. Harvey, and A. J. Mulholland, Benchmarking quantum mechanical methods for calculating reaction energies of reactions catalyzed by enzymes, *PeerJ Phys. Chem.* **2**, e8 (2020).

[21] X. Pan, P. Li, J. Ho, J. Pu, Y. Mei, and Y. Shao, Accelerated computation of free energy profile at ab initio quantum mechanical/molecular mechanical accuracy via a semi-empirical reference potential. ii. recalibrating semi-empirical parameters with force matching, *Phys. Chem. Chem. Phys.* **21**, 20595 (2019).

[22] L. Shen and W. Yang, Molecular dynamics simulations with quantum mechanics/molecular mechanics and adaptive neural networks, *J. Chem. Theory Comput.* **14**, 1442 (2018).

[23] R. W. Zwanzig, High-temperature equation of state by a perturbation method. i. nonpolar gases, *J. Chem. Phys.* **22**, 1420 (1954).

[24] J. Gao, Absolute free energy of solvation from monte carlo simulations using combined quantum and molecular mechanical potentials, *J. Phys. Chem.* **96**, 537 (1992).

[25] R. P. Muller and A. Warshel, Ab initio calculations of free energy barriers for chemical reactions in solution, *J. Phys. Chem.* **99**, 17516 (1995).

[26] M. A. Olsson, P. Söderhjelm, and U. Ryde, Converging ligand-binding free energies obtained with free-energy perturbations at the quantum mechanical level, *J. Comput. Chem.* **37**, 1589 (2016).

[27] M. A. Olsson and U. Ryde, Comparison of qm/mm methods to obtain ligand-binding free energies, *J. Chem. Theory Comput.* **13**, 2245 (2017).

[28] P. Li, X. Jia, X. Pan, Y. Shao, and Y. Mei, Accelerated computation of free energy profile at ab initio quantum mechanical/molecular mechanics accuracy via a semi-empirical reference potential. i. weighted thermodynamics perturbation, *J. Chem. Theory Comput.* **14**, 5583 (2018).

[29] L. Shen, J. Wu, and W. Yang, Multiscale quantum mechanics/molecular mechanics simulations with neural networks, *J. Chem. Theory Comput.* **12**, 4934 (2016).

[30] B. Chehaibou, M. Badawi, T. Bućko, T. Bazhirov, and D. Rocca, Computing rpa adsorption enthalpies by machine learning thermodynamic perturbation theory, *J. Chem. Theory Comput.* **15**, 6333 (2019).

[31] T. Bućko, M. Gešvandnerová, and D. Rocca, Ab initio calculations of free energy of activation at multiple electronic structure levels made affordable: An effective combination of perturbation theory and machine learning, *J. Chem. Theory Comput.* **16**, 6049 (2020).

[32] C. Jarzynski, Targeted free energy perturbation, *Phys. Rev. E* **65**, 046122 (2002).

[33] A. Hahn and H. Then, Using bijective maps to improve free-energy estimates, *Phys. Rev. E* **79**, 011113 (2009).

[34] P. Wirnsberger, A. J. Ballard, G. Papamakarios, S. Abercrombie, S. Racanière, A. Pritzel, D. Jimenez Rezende, and C. Blundell, Targeted free energy estimation via learned mappings, *J. Chem. Phys.* **153**, 144112 (2020).

[35] Z. Zhu, M. E. Tuckerman, S. O. Samuelson, and G. J. Martyna, Using novel variable transformations to enhance conformational sampling in molecular dynamics, *Phys. Rev. Lett.* **88**, 100201 (2002).

[36] G. Papamakarios, E. Nalisnick, D. J. Rezende, S. Mohamed, and B. Lakshminarayanan, Normalizing flows for probabilistic modeling and inference, *J. Mach. Learn. Res.* **22**, 1 (2021).

[37] D. P. Kingma, T. Salimans, R. Jozefowicz, X. Chen, I. Sutskever, and M. Welling, Improved variational inference with inverse autoregressive flow, in *Advances in Neural Information Processing Systems*, Vol. 29, edited by D. Lee, M. Sugiyama, U. Luxburg, I. Guyon, and R. Garnett (Curran Associates, Inc., 2016).

[38] M. Germain, K. Gregor, I. Murray, and H. Larochelle, Made: Masked autoencoder for distribution estimation, in *Proceedings of the 32nd International Conference on Machine Learning*, Proceedings of Machine Learning Research, Vol. 37, edited by F. Bach and D. Blei (PMLR, Lille, France, 2015) pp. 881–889.

[39] See Supplemental Material for (1) detailed derivation of the log likelihood used to learn the FES, its asymptotic properties, and the systematic error on the training set; (2) an estimator for ensemble averages that exploit the mapping function to compute the free energy barriers; (3) simulation and neural network parameters. The Supplemental Material includes Refs. [50–59] and a link to the source code and input files.

[40] J. J. P. Stewart, Optimization of parameters for semiempirical methods v: modification of nddo approximations and application to 70 elements, *J. Mol. Model.* **13**, 1173 (2007).

[41] E. Vanden-Eijnden and F. A. Tal, Transition state theory: Variational formulation, dynamical corrections, and error estimates, *J. Chem. Phys.* **123**, 184103 (2005).

[42] K. M. Bal, S. Fukuhara, Y. Shibuta, and E. C. Neys, Free energy barriers from biased molecular dynamics simulations, *J. Chem. Phys.* **153**, 114118 (2020).

[43] J. Thirman, H. Rui, and B. Roux, Elusive intermediate state key in the conversion of atp hydrolysis into useful work driving the ca2+ pump serca, *J. Phys. Chem. B* **125**, 2921 (2021).

[44] T. Ludwig, A. R. Singh, and J. K. Nørskov, Subsurface nitrogen dissociation kinetics in lithium metal from metadynamics, *J. Phys. Chem. C* **124**, 26368 (2020).

[45] L. Bonati, V. Rizzi, and M. Parrinello, Data-driven collective variables for enhanced sampling, *J. Phys. Chem. Lett.* **11**, 2998 (2020).

[46] P. Ravindra, Z. Smith, and P. Tiwary, Automatic mutual information noise omission (amino): generating order parameters for molecular systems, *Mol. Syst. Des. Eng.* **5**, 339 (2020).

[47] C. X. Hernández, H. K. Wayment-Steele, M. M. Sultan, B. E. Husic, and V. S. Pande, Variational encoding of complex dynamics, *Phys. Rev. E* **97**, 062412 (2018).

[48] C. Wehmeyer and F. Noé, Time-lagged autoencoders: Deep learning of slow collective variables for molecular kinetics, *J. Chem. Phys.* **148**, 241703 (2018).

[49] D. Krause and P. Thörnig, Jureca: Modular supercomputer at jülich supercomputing centre, *Journal of large-scale research facilities* **4**, A132 (2018).

[50] M. R. Shirts and J. D. Chodera, Statistically optimal analysis of samples from multiple equilibrium states, *J. Chem. Phys.* **129**, 124105 (2008).

[51] M. R. Shirts, Reweighting from the mixture distribution as a better way to describe the multistate bennett acceptance ratio, *arXiv:1704.00891 [cond-mat.stat-mech]* (2017).

[52] T. C. Hesterberg, *Advances in importance sampling*, Ph.D. thesis, Standford University (1988).

[53] A. Paszke, S. Gross, F. Massa, A. Lerer, J. Bradbury, G. Chanan, T. Killeen, Z. Lin, N. Gimelshein, L. Antiga, A. Desmaison, A. Kopf, E. Yang, Z. DeVito, M. Raison, A. Tejani, S. Chilamkurthy, B. Steiner, L. Fang, J. Bai, and S. Chintala, Pytorch: An imperative style, high-performance deep learning library, in *Advances in Neural Information Processing Systems 32*, edited by H. Wallach, H. Larochelle, A. Beygelzimer, F. d'Alché-Buc, E. Fox, and R. Garnett (Curran Associates, Inc., 2019) pp. 8024–8035.

[54] D. A. Case, R. M. Betz, D. S. Cerutti, T. E. Cheatham, III, T. A. Darden, R. E. Duke, T. J. Giese, H. Gohlke, A. W. Goetz, N. Homeyer, S. Izadi, P. Janowski, J. Kaus, A. Kovalenko, T. S. Lee, S. LeGrand, P. Li, C. Lin, T. Luchko, R. Luo, B. Madej, D. Mermelstein, K. M. Merz, G. Monard, H. Nguyen, H. T. Nguyen, I. Omelyan, A. Onufriev, D. R. Roe, A. Roitberg, C. Sagui, C. L. Simmerling, W. M. Botello-Smith, J. Swails, R. C. Walker, J. Wang, R. M. Wolf, X. Wu, L. Xiao, and P. A. Kollman, Amber 16, University of California, San Francisco (2016).

[55] G. A. Tribello, M. Bonomi, D. Branduardi, C. Camilloni, and G. Bussi, Plumed 2: New feathers for an old bird, *Comput. Phys. Commun.* **185**, 604 (2014).

[56] R. M. Parrish, L. A. Burns, D. G. Smith, A. C. Simmonett, A. E. DePrince III, E. G. Hohenstein, U. Bozkaya, A. Y. Sokolov, R. Di Remigio, R. M. Richard, *et al.*, Psi4 1.1: An open-source electronic structure program emphasizing automation, advanced libraries, and interoperability, *J. Chem. Theory Comput.* **13**, 3185 (2017).

[57] D. Mendels, G. Piccini, and M. Parrinello, Collective variables from local fluctuations, *J. Phys. Chem. Lett.* **9**, 2776 (2018).

[58] G. Piccini, D. Mendels, and M. Parrinello, Metadynamics with discriminants: A tool for understanding chemistry, *J. Chem. Theory Comput.* **14**, 5040 (2018).

[59] G. Papamakarios, T. Pavlakou, and I. Murray, Masked autoregressive flow for density estimation, arXiv:1705.07057 [stat.ML] (2017).